

Properties of Alfvén waves in ohmic plasma in the TUMAN-3M tokamak

G.I. Abdullina, L.G. Askinazi, A.A. Belokurov, V.A. Kornev, S.V. Krikunov, S.V. Lebedev,
D.V. Razumenko, A.I. Smirnov, A.S. Tukachinsky, N.A. Zhubr

Ioffe Institute, St. Petersburg, Russian Federation

Some properties of Alfvén waves (AWs) in ohmic plasma in the TUMAN-3M tokamak are reviewed in [1 – 4]. Namely, AW location was found to be in the region $r/a < 0.4$ - 0.5 [4], by matching the AW frequency calculated from experimental electron density profile with the experimentally measured one. It was found that the calculated frequency fits well with the experimental one in a relatively wide region $r < 6$ cm, thus pointing on the global nature of the mode. The observed mode was identified as GAE (Global Alfvén Eigenmode), and at the same time, TAE mode (Toroidal Alfvén Eigenmode) was excluded from the list of possible instabilities which could cause the oscillations observed on magnetic probes [1, 2, 4]. It was shown that a deviation of the AW frequency dependence on AW velocity from the linear law in [3] is eliminated if Alfvén velocity is calculated using local values of the plasma density in the propagation region instead of the chord-averaged density. Some suggestions about a role of runaway electrons in AW generation in ohmic plasma are proposed in paper [2].

Array of magnetic probes. Array of magnetic probes in the TUMAN-3M presents 16 magnetic probes located uniformly in single poloidal cross-section. Thus, poloidal mode numbers $m < 8$ can be identified. All magnetic probes are identical and have amplifier's gain $19 \pm 10\%$ in fundamental Alfvén range 0.6 – 2.1 MHz, full frequency range 0.01 – 100 MHz (designed for 250 MHz ADC), ADC sampling frequency 64 MHz.

Short and long Alfvén bursts. Bursting and quasi-continuous Alfvén waves in ohmic plasma [3] seem to have different physical nature. As can be seen from Figure 1, bursting AW or short burst ($t = 73.62$ - 73.67 ms, $f = 0.82$ MHz) appears just after sawtooth crash, while quasi-continuous AW or long burst ($t = 73.90$ - 74.08 ms, $f = 0.80$ MHz) develops at the rise phase of the sawtooth. Amplitude of the short burst is ~ 10 times higher than the long one. Fundamental frequency of both short and long bursts looks unaffected by NBI heating. Bursts under discussion are taken during NBI pulse. Effect of NBI on second and third harmonics of fundamental frequency has not studied yet.

Fundamental frequency and second, third harmonics. Second and third harmonics of the both short and long bursts were observed in some discharges. Third harmonic of the short

burst was observed only on few probes. Second and third harmonics of the long burst have very low amplitudes. Amplitude of short burst second harmonic is approximately ~ 50 times lower than one of fundamental frequency.

Mode structure and temporal evolution of AW.

Mode numbers of AW oscillations were determined by spatial Fourier analysis in cylindrical approximation.

Mode amplitude is given by $I_m = \sqrt{I_1^2 + I_2^2}$, where

$$I_1 = \frac{1}{\pi} \int_0^{2\pi} U(\theta) \cdot \cos(m\theta) d\theta, \quad I_2 = \frac{1}{\pi} \int_0^{2\pi} U(\theta) \cdot \sin(m\theta) d\theta$$

and $m = 0 \dots 7$. Instantaneous values of probe voltages were interpolated by a cubic spline and then this function was employed as $U(\theta)$.

Fundamental frequency of the short burst. Fourier analysis indicates maximum amplitudes for $m = 2, 3$ as shown in Figure 3c. Time evolution of $U(\theta)$ showed that the perturbation is predominantly concentrated in the upper part of plasma cross-section. Figure 3a

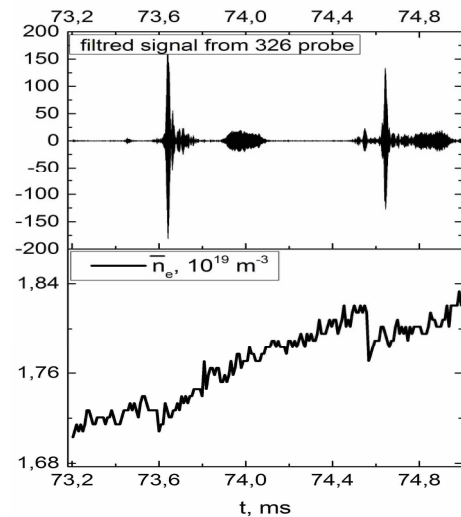


Figure 1. Correlation of short and long bursts with sawtooth activity.

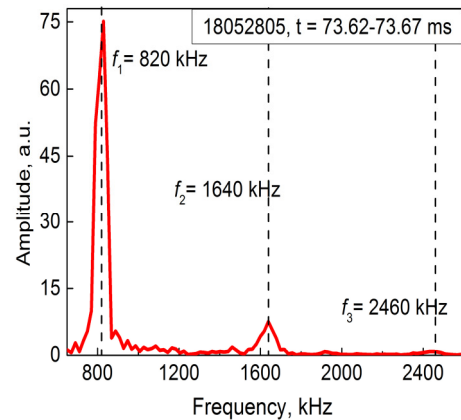
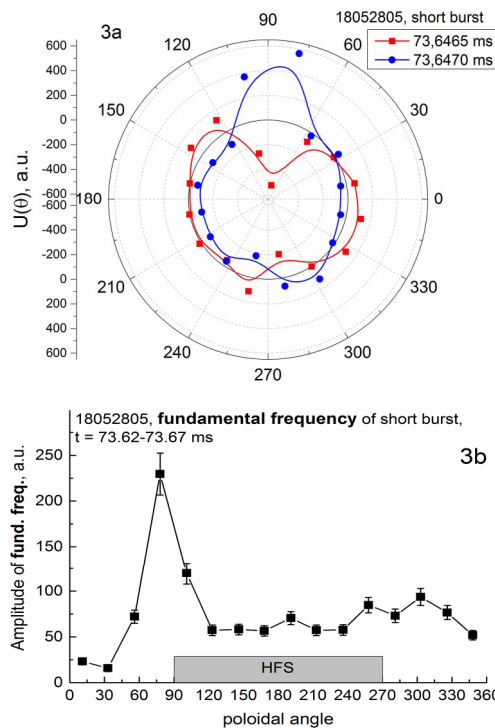
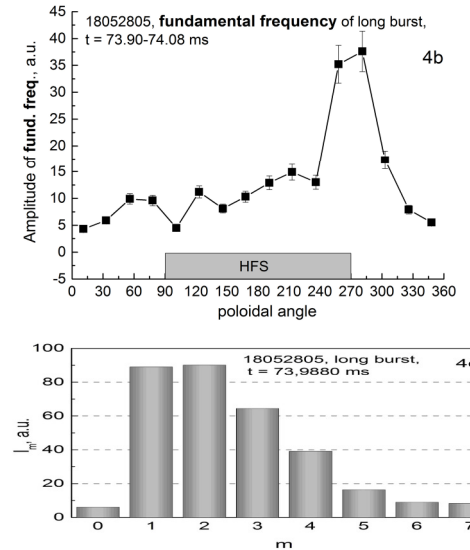
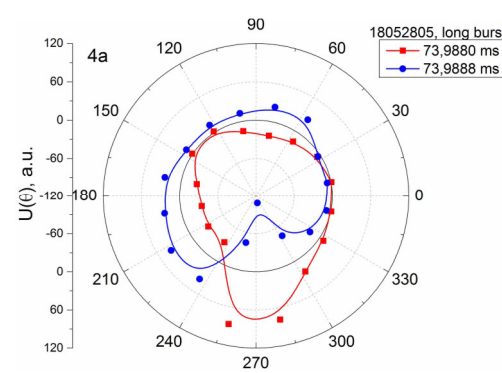
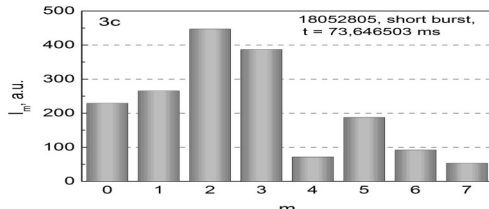


Figure 2. Spectrum of the short Alfvén burst.



demonstrates two such typical shapes of $U(\theta)$, which were repeated over burst duration. Figure 3b illustrates this feature: the amplitude of fundamental frequency over all burst duration at $60 - 90^\circ$ is ~ 4 times higher than the same for the other poloidal angles. Another feature temporal evolution of AW is the absence ballooning or antiballooning character - amplitude of AW is approximately the same on LFS and HFS, see Figures 3a, 3b.

Fundamental frequency of the long burst. Result of Fourier analysis of the long burst is shown in Figure 4c. In contrast to the fundamental frequency of short burst, the maximum perturbation is seen in the



Second harmonic of the short burst. Second harmonic of the short burst ($t = 73.62 - 73.67$ ms, $f = 1.64$ MHz) has a somewhat richer mode structure compared to fundamental frequency of the both short and long bursts. Figure 5c shows maximum amplitude of mode is 4, but the other modes $m = 1 \dots 3$ have high enough amplitudes. It is worth to notice, $m = 5, 6, 7$ make

lower part of cross-section, see Figures 4a, 4b.

Figure 4b shows that the oscillations amplitude in the range $260 - 280$ $^\circ$ is ~ 3.5 times higher than for the rest angles during all the burst duration. The temporal evolution of perturbation shows poloidal symmetry as well (LFS - HFS).

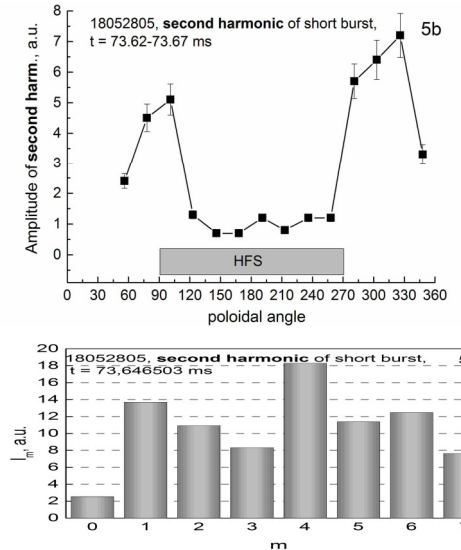
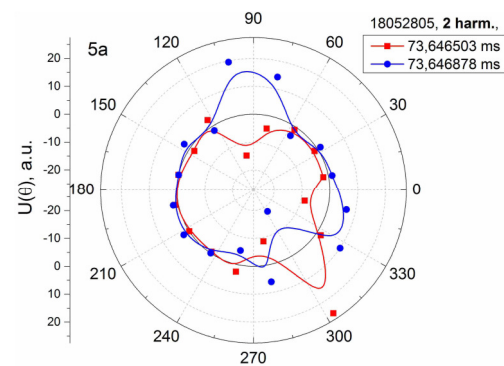


Figure 5 a, b, c. – Results for second harmonic of the short burst fundamental frequency. a – Poloidal distribution of magnetic field perturbation at two time moments. b – Amplitude of perturbation averaged over the burst duration. c – Mode numbers obtained by Fourier analysis.

essential contribution to overall mode structure in contrast to fundamental frequency of the both short and long bursts. Temporal evolution of $U(\theta)$ demonstrates the perturbation location basically at LFS on poloidal range 270-120°, see Figure 5a, 5b. Thus, second harmonic of fundamental frequency of the short burst has a distinct ballooning character.

Impurity influence on Alfvén wave frequency.

The dependence of AW frequency on carbon impurity content has been studied in deuterium plasma. It has been experimentally confirmed that in case of fully ionized carbon, when mass-to-charge ratio is the same for both main (D^+) and impurity (C^{6+}) ions, AW frequency is independent on impurity density [5], and is determined by electron plasma density and main ion mass. Figure 6 demonstrates two spectra of AW burst obtained in deuterium and carbon-contaminated plasmas. This difference in frequencies is due solely to the difference in electron densities, as it was established by estimation of effective ion charge.

Conclusions concerning the mode structure of the short and the long bursts

For the both types of AW bursts a strong poloidal asymmetry (up - down) of the perturbation at fundamental frequency without a pronounced ballooning/ antiballooning effect was observed. This confirms central location of AW. In the case of the short burst a perturbation was predominantly located in the upper part of the plasma core. Contrary, a perturbation was located in the lower part in the long burst case. For the short burst the second harmonic of the fundamental frequency has maximal amplitude at LFS, thus demonstrating ballooning effect. For the both types of the bursts at the fundamental frequency no poloidal rotation was detected.

Acknowledgements

The studies of the Alfvén wave location and the mode structure were supported by Russian Science Foundation (Project # 16-12-10285). The study of Alfvén waves in deuterium plasma with increased carbon impurity content was supported by Ioffe Institute.

References:

- [1] Askinazi L.G. et al 2015 Nucl. Fusion 55 104013
- [2] Tukachinsky A.S. et al 2016 Technical Physics Letters **42** pp 1167-1169
- [3] Lebedev S.V. et al 2016 Proc. 43rd EPS Conf. on Plasma Phys. P5.036
- [4] Abdullina G.I. et al 2018 Technical Physics Letters **44** p 108
- [5] Heidbrink W.W. 2008 Phys. Plasmas 15 055501

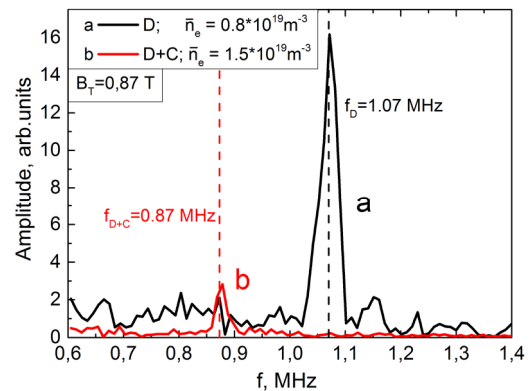


Figure 6. Spectra of AW bursts measured by magnetic probe.